arXiv:cond-mat/0208213v2 [cond-mat.str-el] 19 Aug 2002

The pressure dependence of many-body interactions in the organic superconductor κ-(BEDT-TTF)$_2$Cu(SCN)$_2$: A comparison of high pressure infrared reflectivity and Raman scattering experiments.

R. D. McDonald[1,2,*] and A.-K. Klehe[2] and J. Singleton[1,2] and W. Hayes[2].
[1] *NHMFL, Los Alamos National Laboratory, MS-E536, NM 87545. USA.*
[2] *Clarendon Laboratory, Department of Physics, Parks Road, Oxford, OX1 3PU, UK.*
(Dated: June 13, 2002)

We determine the pressure dependence of the electron-phonon coupling in κ-(BEDT-TTF)$_2$Cu(SCN)$_2$ by comparison of high pressure Raman scattering and high pressure infrared (IR) reflectivity measurements. The Raman active molecular vibrations of the BEDT-TTF dimers stiffen by 0.1-1 %GPa^{-1}. In contrast, the corresponding modes in the IR spectrum are observed at lower frequency, with a pressure dependence of 0.5-5.5 %GPa^{-1}, due to the influence of the electron-phonon interaction. Both dimer charge-oscillation and phase-phonon models are employed to extract the pressure dependence of the electron molecular-vibration coupling for these modes. Analysis of our data suggests that the reduction of electron-phonon coupling under pressure does not account for the previously observed suppression of superconductivity under pressure and that electron-electron interactions may contribute significantly to the pairing mechanism.

I. INTRODUCTION

κ-(BEDT-TTF)$_2$Cu(SCN)$_2$ is one of the best characterized organic superconductors[1]. It is a highly anisotropic material with a quasi-two dimensional band structure, whose Fermi-surface topology has been determined by magnetotransport experiments[1,2]. At ambient pressure κ-(BEDT-TTF)$_2$Cu(SCN)$_2$ is a superconductor with a transition temperature of $T_c \simeq 10.4$ K. T_c decreases upon the application of pressure until, at pressures P exceeding 0.5 GPa, superconductivity is fully suppressed[2,3,4]. The quasiparticle effective mass, m^*, derived from magnetic quantum oscillation measurements, decreases linearly with pressure up to 0.5 GPa; above this pressure the magnitude of $\mathrm{d}m^*/\mathrm{d}P$ is strongly reduced[2]. The effective mass measured in this fashion includes contributions from both electron-phonon and electron-electron interactions [5].

In contrast, the optical mass, m_{opt}, extracted from a sum over the optical conductivity, decreases approximately linearly throughout the above pressure range[6]. This mass is thought to be dominated by intraband electronic processes, reflecting the band mass without renormalization by electron-electron and electron-phonon interactions[5,7]. The coincidence of a 'kink' in the pressure dependence of m^* with the pressure above which superconductivity is suppressed and the absence of a 'kink' in the pressure dependence of m_{opt}, suggests that the interactions parameterized by m^* maybe associated with the superconductivity.

The key question to address is the effect of these interactions, *i.e.* what is the dominant pairing mechanism for superconductivity in this material? In this paper we compare infrared (IR)[6,8] and Raman scattering[9] measurements under pressure to determine the role of the electron-phonon interaction. This is possible because the IR measurement probes the molecular vibrations dressed by the electron-phonon interaction[10,11], whereas non-resonant Raman measurements probe the bare mode frequencies[10,12]. The primary effect of the electron-phonon interaction is to soften the IR modes with respect to the Raman modes, as illustrated in Figure 1.

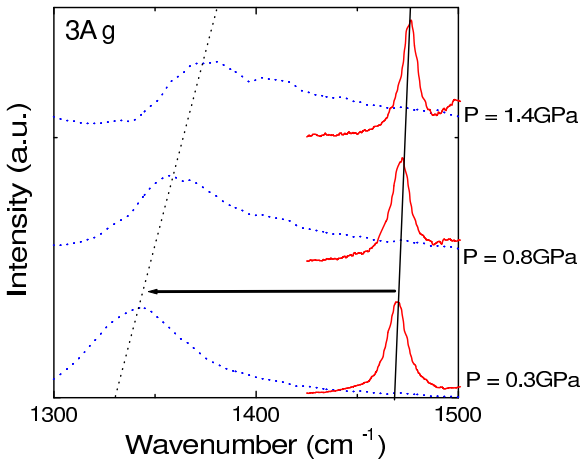


FIG. 1: The spectral region containing the 3A$_g$ molecular vibration, Raman spectra (solid lines) and Infrared spectra with polarization parallel to the crystallographic *b*-axis (dotted lines), for a selection of pressures at room temperature. The spectra are offset for clarity and the vertical lines are a guide to the eye. Note the substantial softening effect of the increased electron-phonon interaction on the IR spectra with respect to the Raman spectrum.

There are two approaches to modelling the electron-molecular vibration coupling interaction and associated mode softening in organic charge transfer systems, the "phase-phonon" theory and the "dimer charge-oscillation" model. The phase-phonon theory approaches the problem from an electron band approximation where

the charge carriers are naturally delocalized. The alternative dimer charge-oscillation theory is formulated in real space such that the electronic behaviour is implicitly localized. In reality the electronic properties of κ-(BEDT-TTF)$_2$Cu(SCN)$_2$ are somewhere between the extremes of a localized and itinerant system[1]. For this reason we apply both the dimer charge-oscillation and phase-phonon models to analyze the data.

This paper is organized as follows. In Section II we describe the vibrational spectra of κ-(BEDT-TTF)$_2$Cu(SCN)$_2$ as observed by both non-resonant Raman scattering and polarized IR reflectivity. Section III describes the methods of analysis, specifically how the pressure dependence of the electron-phonon coupling is extracted. The first subsection of the Discussion, Section IV A, contains a comparison of the quasiparticle masses that result from the different methods of analysis. Subsequently, in Section IV B, in light of the pressure dependence of the electron-phonon coupling, the implications for the superconducting pairing mechanism are discussed. Conclusions are summarized in Section V.

II. DESCRIPTION OF THE OBSERVED VIBRATIONAL MODES.

Four modes are observed in both the high-pressure room-temperature Raman and IR spectra (see Figures 2 and 3 and Table I). They are labeled with subscripts indicating the atoms/bond predominantly involved in the vibration[13]. In order of increasing frequency they are the C-S mode originating from the BEDT-TTF 60B$_{3g}$ asymmetric vibration, the central C=C mode originating from the BEDT-TTF 3A$_g$ symmetric vibration and two Cu(SCN)$_2$ anion modes. Determining the pressure dependence of the central C=C mode in the IR spectrum is not straightforward due to the overlap of several modes with varying pressure dependences. In a recent publication[14], IR spectra from the deuterated salt have been used to model this Fermi resonance and extract the linear pressure dependence of the overlapping modes (the central C=C mode and two C-H modes). The IR and Raman frequencies and the first order pressure dependence of all modes discussed here are given in Table I.

The Cu(SCN)$_2$ anion modes do not exhibit any evidence of electron-phonon coupling, *i.e.* the difference between the infrared and Raman frequencies for the anion modes is accounted for by purely vibrational coupling[9]. The zone center frequency separation, $\Delta\omega_s$, between the symmetric (Raman active) and antisymmetric (infrared active) combinations of the molecular vibrations is determined by the frequency of the optical branch of the lattice modes[9,15]. The larger observed $\Delta\omega_s$ for the anion mode in the b-axis response, for which the lattice mode is stiffer (see Table I), is a further confirmation of the lattice mode assignment given in[9].

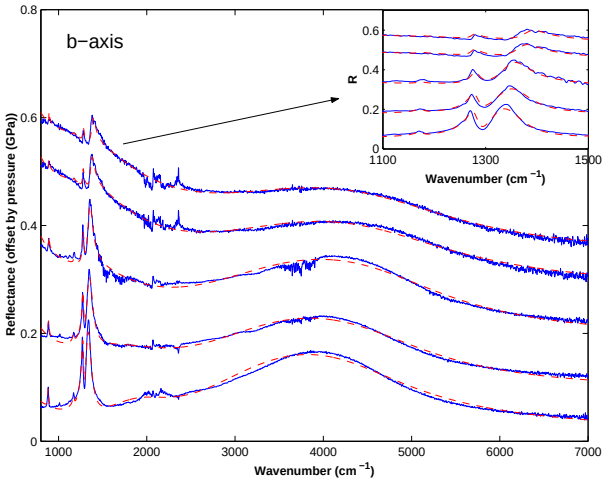


FIG. 2: The room temperature diamond/sample IR reflectance offset by pressure for polarization parallel to the b-axis. Measurement (solid lines) and phase-phonon fit (dashed lines). The inset magnifies the spectral region containing the C=C mode.

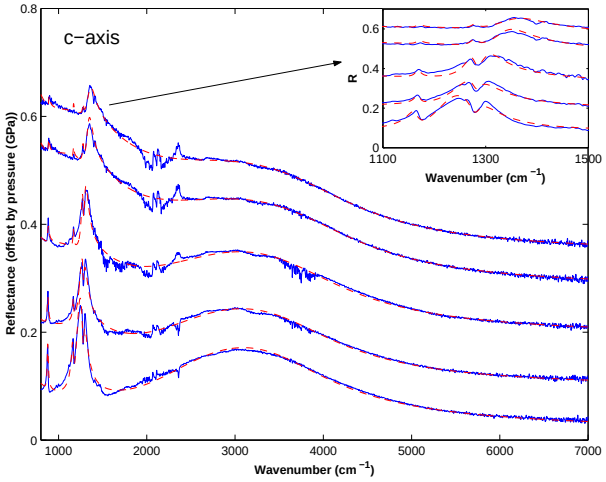


FIG. 3: The room temperature diamond/sample IR reflectance offset by pressure for polarization parallel to the c-axis. Measurement (solid lines) and phase-phonon fit (dashed lines). The inset magnifies the spectral region containing the C=C mode.

III. ANALYSIS.

Electron-molecular vibration coupling can be characterized by a set of linear coupling constants, g_α, which parameterize the interaction between the α^{th} normal mode, of frequency ω_α, and the molecular orbital in which the radical electron or hole resides[16]. For a donor molecule g_α is the rate of change of the energy of the highest occupied molecular orbital with respect to the normal mode coordinate, Q_α,[16]

$$g_\alpha = \frac{\partial \mathrm{E}}{\partial Q_\alpha}. \qquad (1)$$

Mode	Assignment	Raman		Infrared b-axis		Infrared c-axis	
	[13]	cm^{-1}	$+(\%GPa^{-1})$	cm^{-1}	$+(\%GPa^{-1})$	cm^{-1}	$+(\%GPa^{-1})$
ω_{CT}	.....	.....	.....	2910	+ 4.0	2390	+ 4.0
ω_{CS}	B_{3g}	886.2	+ 0.85	883.5	+ 0.71	873.6	+ 1.0
ω_{CC}	A_g	1467.7	+ 0.4	1290	+ 2.5	1210	+ 5.5
ω_{CH_1}	B_{3u}	.....	.....	1181	+ 0.5	1177	+ 0.5
ω_{CH_2}	B_{1u}	.....	.....	1290	+ 0.5	1281	+ 0.5
ω_{anion1}	CN	2064.6	+ 0.1	2067.4	+ 0.1	2065.6	+ 0.15
ω_{anion2}	CN	2106.3	+ 0.2	.....	.....	2109.3	+ 0.2

TABLE I: Raman and IR frequencies and pressure shifts taken from[6,9,14].

To obtain these coupling constants experimentally, an appropriate model has to be applied to the data. Two alternative approaches exist in the literature: the "phase-phonon" theory and the "dimer charge-oscillation" model. Both theories were initially developed by Rice[12,17] to model the infrared spectrum of semiconducting organic charge-transfer systems. However, they have also been applied to a range of reduced dimensionality organic charge transfer salts, including metallic systems[10,16,18,19,20,21,22].

The phase-phonon theory approaches the problem from an electron band approximation where the charge carriers are naturally delocalized. A potential disadvantage of this approach is that it is a one-electron theory, *i.e.* all electron-electron correlation effects have to be included within an effective mass approximation[16].

The alternative dimer charge-oscillation theory is formulated in real space but is limited to a finite number of molecules. The infrared response of the system is calculated from a superposition of the isolated units with no significant charge transfer between the units. For κ-phase BEDT-TTF salts the approximation is that the charge carriers are predominantly localized on the dimers which are weakly interacting with each other. Although this implies an insulating system, with the response of delocalized charge carriers parameterized separately, electron-electron correlations such as the onsite Coulomb repulsion can be included explicitly[19].

A. The dimer charge-oscillation model.

This subsection outlines the derivation of the dimer charge-oscillation model[12,19]. Not only does this aid discussion relating to the validity of applying this model to κ-(BEDT-TTF)$_2$Cu(SCN)$_2$, but it also lends theoretical weight to the concept of electron coupling to the antisymmetric combinations of molecular vibrations and not to the symmetric combinations. This concept is the key to comparing Raman and infrared data in order to probe the electron-phonon coupling.

Each dimer unit is modelled by the following Hamiltonian ($\hbar = 1$)[12,19],

$$H = H_e + H_\nu + \sum_{\alpha,j} n_j g_\alpha Q_{\alpha,j}. \quad (2)$$

The first two terms describe, respectively, the electronic states and the molecular vibrations in the absence of vibrational coupling; j labels the molecule and α the normal mode of vibration. Rice's formulation includes only the totally symmetric (A_g) molecular modes. However, later theories have extended the theory to internal modes of other symmetries[23].

The electronic term, H_e, is of the form,

$$H_e = \sum_{j=1:2} E_0 n_j + V, \quad (3)$$

where $n_j = \sum_\sigma c^\dagger_{j,\sigma} c_{j,\sigma}$ is the occupation number operator for the molecular orbital of energy E_0. $c^\dagger_{j,\sigma}$ and $c_{j,\sigma}$ are the Fermion creation and annihilation operators for an electron of spin σ[24,25]. The exact form of the potential term, V, is arbitrary.

The phonon term, H_ν, is of the conventional form for a harmonic oscillator of frequency ω_α[19,24,25],

$$H_\nu = \sum_{j,\alpha} \omega_\alpha (b^\dagger_{j,\alpha} b_{j,\alpha} + \frac{1}{2}), \quad (4)$$

where $b^\dagger_{j,\alpha}$ and $b_{j,\alpha}$ are the Boson creation and annihilation operators. Their sum is the displacement operator for the α^{th} normal mode and their difference is its momentum operator[25], *i.e.*

$$Q_{j,\alpha} \propto (b^\dagger_{j,\alpha} + b_{j,\alpha}). \quad (5)$$

Because the dimer has been chosen as the base unit for this system it is appropriate to introduce dimer-mode coordinates

$$s_\alpha = \frac{1}{\sqrt{2}}(Q_{1,\alpha} + Q_{2,\alpha}) \quad (6)$$

and

$$q_\alpha = \frac{1}{\sqrt{2}}(Q_{1,\alpha} - Q_{2,\alpha}) \quad (7)$$

which are symmetric and antisymmetric combinations of the molecular-mode coordinates respectively.

The third term in the Hamiltonian is a linear perturbation arising from the electron-molecular vibration coupling. Commutation of the dimer-mode coordinates with the system Hamiltonian yields two equations of motion for the α^{th} molecular mode[19,26]

$$\langle \ddot{s}_\alpha \rangle + \omega_\alpha^2 \langle s_\alpha \rangle = -\sqrt{2} g_\alpha \omega_\alpha \langle n_1 + n_2 \rangle \tag{8}$$

and

$$\langle \ddot{q}_\alpha \rangle + \omega_\alpha^2 \langle q_\alpha \rangle = -\sqrt{2} g_\alpha \omega_\alpha \langle n_1 - n_2 \rangle. \tag{9}$$

The right-hand side of the equation of motion for the symmetric combination of molecular modes is dependent on the total charge density, $\langle N_{\text{tot}} \rangle = \langle n_1 + n_2 \rangle$, which for an isolated dimer is constant, *i.e.* the symmetric combination of modes is uncoupled from the electron system. Their unperturbed frequencies, ω_α, are therefore obtained experimentally from Raman scattering experiments[12].

The right-hand side of the equation of motion for the antisymmetric combination of molecular modes is dependent upon the electric dipole moment of the dimer, $\langle \mathbf{p} \rangle = \frac{1}{2} e \mathbf{a} \langle n_1 - n_2 \rangle$, where e is the electron charge and $\mathbf{a}$ is a vector perpendicular to the interface between the two molecules, whose magnitude is of the order of the intermolecular separation. Therefore the antisymmetric combination of modes is directly coupled to the electron dipole moment and is hence infrared active[12]. For a simple two-state electron Hamiltonian these modes couple to the charge-transfer excitation between the ground and excited states, $|1\rangle \rightarrow |2\rangle$.

Because the interaction part of the Hamiltonian is of the form

$$H_i = \sum_k \rho_k \varphi_k, \tag{10}$$

where φ is a scalar potential, the expectation value of the operator ρ which characterizes the response of the system to the perturbation may be calculated using linear response theory[26,27,28]. The ground state expectation value of the Fourier components of the dipole moment, $\langle \mathbf{p}(\omega) \rangle$, and hence the complex conductivity, $\sigma(\omega)$, of the dimer charge-oscillation system are given by the linear-response function[12,26],

$$\sigma(\omega) = -\mathrm{i}\omega \frac{e^2 \mathbf{a}^2}{2\mathcal{V}} \left(\frac{1}{\chi(\omega)} - \sum_\alpha \frac{g_\alpha^2 \omega_\alpha}{\omega_\alpha^2 - \omega^2 - \mathrm{i}\omega\gamma_\alpha} \right)^{-1}. \tag{11}$$

Here $\mathcal{V}$ is the molecular volume and $\chi(\omega)$ the reduced charge transfer polarizability;

$$\chi(\omega) = |\langle 2|\mathbf{p}|1\rangle|^2 \frac{2\omega_{\text{CT}}}{\omega_{\text{CT}}^2 - \omega^2 - \mathrm{i}\omega\Gamma}, \tag{12}$$

where $\langle 2|\mathbf{p}|1\rangle$ is the matrix element for the charge-transfer transition of frequency ω_{CT}. The electron and phonon damping factors, Γ and γ_α, are introduced phenomenologically to account for the observed infrared linewidths. It should be noted that this perturbation will alter the frequency at which the coupled molecular vibrations are observed in the infrared spectrum; for $\omega_\alpha > \omega_{\text{CT}}$ their frequencies will be red shifted[19].

The crux of this subsection is to address how the dimer charge-oscillation model may be used to extract the electron-phonon coupling constants by means of experiment. Several approaches have been proposed to reduce the possible parameter space encountered when fitting infrared reflectance data with this model. It has been noted[16] that the inverse of the real part of the conductivity, calculated using equation 11, consists of a constant background arising from the charge-transfer band with peaks occurring at the unperturbed frequencies of the vibrational modes, ω_α. In principal, if this model accurately describes the data, Kramers-Kronig analysis could be used to calculate $\text{Re}\left(\frac{1}{\sigma(\omega)}\right)$ and thus determine the bare-mode frequencies. However, because of uncertainties in the Kramers-Kronig procedure[6] Raman measurement of the unperturbed frequencies are more reliable.

Analysis of the poles and zeros of the response function (Equation 11) leads to the following approximate relation between the observed frequency of the infrared phonon bands, Ω_α, their unperturbed frequencies, ω_α, the frequency of the coupling charge-transfer band, ω_{CT}, and the dimensionless electron molecular vibration coupling constants, λ_α[10,20];

$$\frac{\omega_\alpha^2 - \Omega_\alpha^2}{\omega_\alpha^2} = \lambda_\alpha \frac{\omega_{\text{CT}}^2}{\omega_{\text{CT}}^2 - \omega_\alpha^2}. \tag{13}$$

This expression is valid if the bare frequencies of the modes are well separated from each other or λ_α sufficiently small so that each mode may be treated individually. For κ-(BEDT-TTF)$_2$Cu(SCN)$_2$ the two observed modes with a finite λ_α (the C=C and C-S modes) are well separated from each other. Note that the C=C mode overlaps with two C-H modes as discussed in Section II; however the lack of spectral weight associated with the C-H modes[14] indicates that their electron-phonon coupling is negligable in this case. Within the dimer charge oscillation model λ_α is related to g_α via[29]

$$\lambda_\alpha = \frac{2 g_\alpha^2}{\omega_\alpha \omega_{\text{CT}}}. \tag{14}$$

B. The electron-phonon coupling constant and its pressure derivative derived from the dimer charge-oscillation model.

Equation 13 is used to calculate an electron-phonon coupling constant, λ_α, for each mode from its Raman and infrared frequencies, ω_α and Ω_α, given knowledge of the energy, ω_{CT}, of the coupling charge-transfer band[10,20] (see Table II). The dominant source of error in this calculation is due to the width of the charge-transfer band.

There also exists the possibility of coupling to two different charge-transfer transitions. The C=C mode, being an antisymmetric combination of A_g molecular modes, couples to the intradimer charge transfer[23]. It has been calculated,[23] however, that the antiphase combination of B_{3g} molecular modes couples to charge transfer perpendicular to the intradimer direction. This suggests that the C-S mode couples to transitions between the lower and upper branches of the same band, not interband electronic transitions. However, it should be noted that the electron-phonon coupling constants for the C-S mode have been calculated using the same $\omega_{\rm CT}$ as the C=C mode because it is impossible to distinguish the contributions to the infrared spectrum from different transitions.

The pressure derivative of Equation 13,

$$\frac{\mathrm{d}\ln\lambda_\alpha}{\mathrm{d}P} = 2\frac{\Omega_\alpha^2}{\omega_\alpha^2-\Omega_\alpha^2}\left[\frac{\mathrm{d}\ln\omega_\alpha}{\mathrm{d}P}-\frac{\mathrm{d}\ln\Omega_\alpha}{\mathrm{d}P}\right]$$

$$+2\frac{\omega_\alpha^2}{\omega_{\rm CT}^2-\omega_\alpha^2}\left[\frac{\mathrm{d}\ln\omega_{\rm CT}}{\mathrm{d}P}-\frac{\mathrm{d}\ln\omega_\alpha}{\mathrm{d}P}\right], \qquad (15)$$

has a weaker dependence on the value of $\omega_{\rm CT}$. However the dominant source of error in Equation 15 arises from the difficulty in determining an accurate pressure dependence of the broad charge-transfer band. Fitting the infrared reflectance data with a simple Drude-Lorentz model[6] provides an estimate for the pressure dependance of $\omega_{\rm CT}$. Using a value of 4±4 %GPa^{-1} for both *b*- and *c*-axes[6], results in an error in the pressure derivative of the coupling constant for the C=C mode of ±3.5 %GPa^{-1} for the *b*-axis and ±5 %GPa^{-1} for the *c*-axis. The error in the pressure derivative of the coupling constant for the C-S mode is larger (8 %GPa^{-1} for the *b*-axis and 28 %GPa^{-1} for the *c*-axis) because $\lambda_{\rm CS}$ is so small.

Mode	λ_b	$\frac{\mathrm{d}\ln\lambda_b}{\mathrm{d}P}$ %GPa^{-1}	λ_c	$\frac{\mathrm{d}\ln\lambda_c}{\mathrm{d}P}$ %GPa^{-1}
$\omega_{\rm CS}$	0.01(1)	47.9	0.02(1)	-11.1
$\omega_{\rm CC}$	0.17(1)	-11.9	0.20(1)	-17.3
$\omega_{\rm anion1}$	0	0	0	0
$\omega_{\rm anion2}$	.....	.....	0	0

TABLE II: dimensionless electron-phonon coupling constants and their pressure derivatives calculated using the dimer charge-oscillation model. Note in this table the ω subscript referes to the mode and the λ subscript to the polarization direction.

Because the dimer charge-oscillation model is formulated for a localized system, λ_α calculated in this manner parameterizes the strength of interaction between the phonons and the intradimer charge transfer. On the other hand the electron-phonon coupling constant associated with phonon-mediated superconductivity parameterizes the strength of interaction between the phonons and the delocalized charge carriers. Therefore to use this model to draw any conclusions regarding the superconducting mechanism requires the assumption that the electron-phonon coupling for the intradimer charge transfer will, to first order, have the same pressure dependence as the electron-phonon coupling for the interdimer charge transfer. This assumption is reasonable because it is the same molecular orbitals that are responsible for intra- and interdimer wave function overlap. At the Γ-point (the long wavelength limit) neighboring dimers vibrate in phase[30] and as a result, an antiphase combination of molecular vibrations that modulates the intradimer wavefunction overlap will also modulate the interdimer wavefunction overlap.

C. The phase-phonon model.

Phase-phonon theory essentially describes the same phenomenon as the dimer charge-oscillation theory (see equation 2). However, because it is formulated in reciprocal space the model is easily extended to metallic systems. This model is not just limited to the dimer unit, but attributes the infrared activity of the coupled phonon modes to phase oscillations of the spatial charge density, induced by the electron-phonon interaction[17].

The system Hamiltonian is similar to that used in the dimer charge-oscillation theory, and includes an electronic term, $H_{\rm e}$, a phonon term, H_ν, and a linear coupling term, $H_{\rm i}$.

$$H = H_{\rm e} + H_\nu + \frac{1}{\sqrt{\mathtt{N}}}\sum_{\alpha,q} g_\alpha Q_\alpha(q)\rho_{-q}. \qquad (16)$$

The electronic terms has essentially the same form as (3),

$$H_{\rm e} = \sum_{k,\sigma} E_k c^\dagger_{k,\sigma} c_{k,\sigma} + V(\rho_{q_0}+\rho_{-q_0}), \qquad (17)$$

except that the operators create or annihilate a particle in a *k*-state, not at a real space location, *i.e.* it describes a system of conduction electrons moving in a weak periodic potential, V, of wavevector q_0. The operator $\rho_q = \sum_k c^\dagger_{k+q} c_k$ creates an electronic-density fluctuation of wavevector q.

The phonon term is identical to that used in the dimer-charge model except the phonon operators also act on *k*-states. The electron-molecular vibration coupling is included as a linear perturbation, in this case linking the Fourier transform of the mode displacement vector, $Q_\alpha(q) \propto (b_\alpha(q) + b^\dagger_\alpha(-q))$, to an electronic density fluctuation of the same wavevector, q.

$$H_i = \frac{1}{\sqrt{\mathtt{N}}}\sum_{\alpha,q,k} g_\alpha c^\dagger_{k+q} c_k (b_\alpha(q) + b^\dagger_\alpha(-q)). \qquad (18)$$

$\mathtt{N}$ is the density of conduction electrons.

For the case initially considered by Rice,[17] $q_0 = 2k_F$ (twice the Fermi wavevector) such that the periodic

potential induces the conduction electrons to condense into a charge-density-wave state. However, the derivation that follows is equally applicable to a metallic system. The frequency-dependent conductivity for an insulating system is due simply to interband electronic transitions[31],

$$\sigma(\omega) = \frac{\omega_{\rm p}^2}{{\rm i}\omega}\left[f(x) - f(0)\right], \tag{19}$$

where the plasma frequency, $\omega_{\rm p}$, parameterizes the band curvatures. $f(0) = 1$ and

$$f(x) = \frac{\left[{\rm i}\pi + \ln\left(\frac{1-S}{1+S}\right)\right]}{2Sx^2} \tag{20}$$

where $S = \sqrt{1-\frac{1}{x^2}}$ and $x = \frac{\omega}{2\Delta_0}$ with Δ_0 equal to the band gap. Including the electron-phonon coupling modulates the onsite electron energy and hence the band gap, so that $\Delta = \Delta_0 + \sum_\alpha \Delta_\alpha e^{{\rm i}\phi_\alpha}$, where Δ_α and ϕ_α are the amplitude and phase respectively of the distortion potentials which are proportional to g_α. The single electron contributions to $\sigma(\omega)$ are of the same form as the uncoupled case but with $x = \frac{\omega}{2\Delta}$. In addition to the single-electron contributions there are collective contributions associated with oscillations in the phases, ϕ_α, of the combined lattice-charge distortions. Collective modes associated with oscillations in amplitude, Δ_α, also occur: however, they preserve dipole moment and hence do not contribute to the dielectric response[17,21].

Including the collective mode contribution, the frequency-dependent conductivity is given by[17]

$$\sigma(\omega) = -\frac{\omega_{\rm p}^2}{{\rm i}\omega}\left[f(x) - f(0) - x^2(f(x))^2\lambda D_\phi(x)\right]. \tag{21}$$

D_ϕ is a phonon-like propagator for the phase oscillations given by

$$\frac{1}{D_\phi} = \frac{1}{D_0} + 1 - \frac{\Delta_0}{\Delta} + \lambda x^2 f(x). \tag{22}$$

D_0 is the same single-phonon propagator used in the dimer charge-oscillation model,

$$D_0 = -\sum_\alpha \frac{\lambda_\alpha}{\lambda}\frac{\omega_\alpha^2}{\omega_\alpha^2 - \omega^2 - {\rm i}\omega\gamma_\alpha}. \tag{23}$$

In the phase-phonon model the dimensionless coupling constant, λ is related to g_α via

$$\lambda_\alpha = \frac{\mathtt{N}(k_F)g_\alpha^2}{\omega_\alpha}, \tag{24}$$

where $\mathtt{N}(k_F)$ is the density of electron states at the Fermi-surface and the total electron-phonon coupling constant, $\lambda = \sum_\alpha \lambda_\alpha$[16].

It is necessary to include an electronic damping term, Γ, to account for the finite electron lifetime if the model is to be applied to a metallic system, *i.e.* when a large plasma frequency is required to account for the intraband processes. In this case $f(x)$ is replaced by $f(x + {\rm i}\Gamma)$[32].

For $\omega_\alpha < 2\Delta$ decay of the collective mode via excitation of a real electron-hole pair is energetically impossible. As a result each mode contributes a sharp absorption band to the infrared spectrum whose width is determined solely by the lineshape of the uncoupled phonon mode. For $\omega_\alpha > 2\Delta$ the collective modes become damped via electron-hole excitation, appearing as indentations in the electronic background[21].

D. The electron-phonon coupling constant and its pressure derivative derived from the phase-phonon model.

The electron-phonon coupling constant that occurs in the phase-phonon model parameterizes the degree to which each molecular vibration modulates the energy of the electronic band structure, *i.e.* it parameterizes both the inter- and intraband electron-phonon coupling.

To calculate λ_α for each mode the full diamond/sample IR reflectance spectrum[6] is fitted at each pressure-point. The model function for this fit consists of the phase-phonon model plus a high frequency contribution to the dielectric constant, ε_∞, and a highly damped Lorentzian oscillator to account for the anomalous electronic damping at room temperature[33]. The plasma frequency, electronic damping and perturbed and unperturbed interband transition frequencies are treated as free parameters. As with a simple Drude response, the plasma frequency parameterizes the density of states and band curvature, but in this case the electronic damping controls the relative spectral weights of the inter- and intraband processes.

Four phase-phonon collective modes ($\alpha = 1 \rightarrow 4$) are used to model the spectrum, one for the C-S mode and three for the C=C mode and its Fermi resonance with the C-H modes. It was found that the line shape of the Fermi resonance could be reproduced in an analogous manner to the Green's function model used in[14], *i.e.* with one strongly coupled C=C mode and two C-H modes with negligible electron-phonon coupling (see the inset of Figures 2 and 3). The pressure dependence of the modes' Raman frequencies and the pressure dependence of the dips from the Green's function model were used to fix the frequency of the collective modes. Their damping and coupling strengths were left as free parameters, however.

In this model the degree of mode softening associated with the electron-phonon coupling is predominantly parameterized by the perturbation to the interband transition, *i.e.* the difference between the perturbed and unperturbed transition frequencies. The coupling strength, λ_α, controls the mode softening to a lesser extent, mainly parameterizing the spectral weight associated with each mode. Because of this, correctly determining λ relies on accurately modelling the background reflectance in the

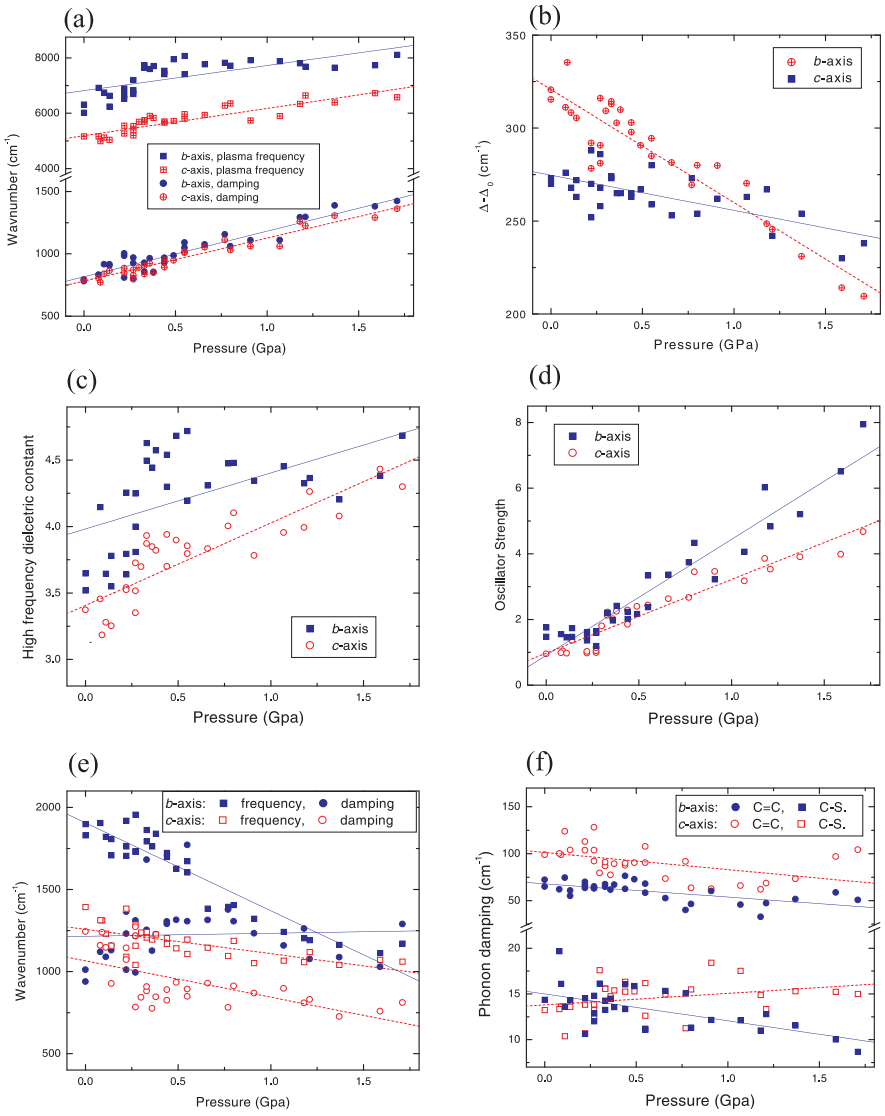


FIG. 4: The pressure dependence of the free parameters of the phase-phonon model. Note that the linear fits indicate the first order pressure dependence used for the batch fitting procedure. Solid lines and symbols are used for polarization parallel to the b-axis and dashed lines and hollow symbols for polarization parallel to the c-axis. (a) the plasma frequency and electronic damping. (b) the difference between the perturbed and unperturbed interband transition frequency. (c) the high frequency dielectric constant. (d) the strength of the Lorentzian oscillator. (e) the frequency and damping of the Lorentzian oscillator. (f) the damping of the C-S and C=C modes.

spectral region containing the modes. To this end, it was found that including the heavily damped Lorentzian to help model this material's anomalous Drude response drastically reduced the scatter in the λ data. The three parameters describing the Lorentzian, ω_e,γ_e and $\Delta\varepsilon_e$, were also free.

The lineshape of the anion modes is most accurately reproduced using uncoupled Lorentzian oscillators. Owing to their lack of electron coupling and their limited contribution to the spectrum, parameters describing them were not included in this model. Figures 2 and 3 indicate the quality of the fits for a representative selection of pressures.

Manually fitting 31 spectra, each consisting of 3300

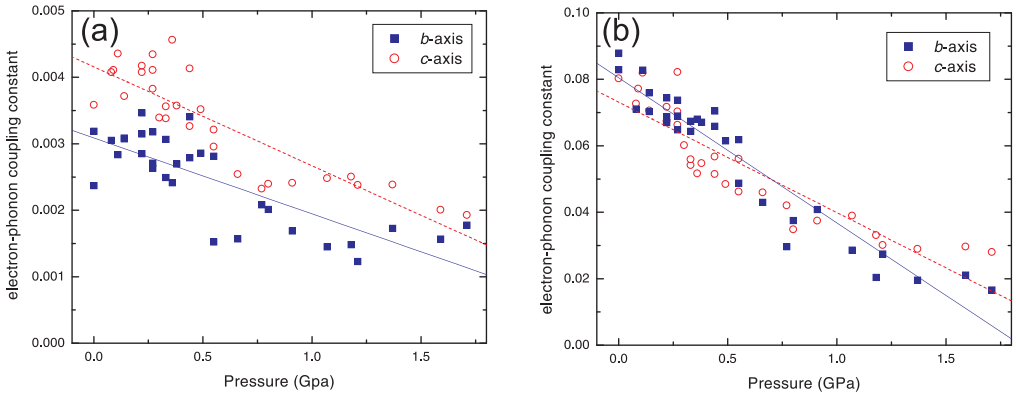


FIG. 5: The pressure dependence of the electron-phonon coupling constant. Solid squares and lines for polarization parallel to the b-axis and hollow circles and dashed lines for polarization parallel to the c-axis. (a) for the C-S mode and (b) for the C=C mode.

Parameter	b-axis cm^{-1}	value $+\%GPa^{-1}$	c-axis cm^{-1}	value $+\%GPa^{-1}$
ω_p	(6816±120)	+(13±2)	(5190±66)	+(19±2)
Γ	(815±16)	+(45±3)	(781±12)	+(45±3)
Δ_0	(1132±13)	+(10±2)	(743±7)	+(17±2)
Δ	(1407±14)	+(6±2)	(1064±8)	+(6±1)
$\Delta-\Delta_0$	(275±3)	-(7±2)	(320±3)	-(19±2)
γ_{CS}	(15±0.5)	-(26±7)	(13±0.5)	+(8±8)
γ_{CC}	(68±2)	-(21±5)	(101±5)	-(18±6)
ω_e	(1905±25)	-(28±2)	(1257±21)	-(12±2)
γ_e	(1214±51)	+(2±6)	(1065±38)	-(21±2)
		$+\%GPa^{-1}$		$+\%GPa^{-1}$
$\Delta\varepsilon_e$	(0.90±0.15)	+(388±22)	(1.00±0.10)	+(272±15)
ε_∞	(3.9±0.1)	+(11±3)	(3.4±0.1)	+(18±3)
λ_{CS}	$(3\times10^{-3}\pm1\times10^{-4})$	-(32±5)	$(3\times10^{-3}\pm1\times10^{-4})$	-(25±4)
λ_{CC}	(0.080±0.002)	-(55±4)	(0.073±0.002)	-(44±3)

TABLE III: Phase phonon model parameters and their first order pressure shifts.

data points, with an expression containing 12 free parameters, for each polarization, is both immensely time consuming and subject to systematic human error. To avoid this a batch fitting procedure was employed. It consists of accurately fitting a limited number of data sets to determine approximate trends for the free parameters. These are then used as the the starting conditions for an automatic least-squares fitting procedure of all data sets. Each fit is then checked visually for acceptance of its parameters.

The value of the free parameters and their first order pressure shifts extracted from Figures 4 and 5 are contained in Table III. The difference in the values of the coupling constants, λ, obtained from the phase-phonon model (TABLE III) and the dimer charge-oscillation model(TABLE II) are predominantly due to the different values for the interband transition used in each calculation.

IV. DISCUSSION.

As well as vibrational features the room temperature IR spectrum of κ-(BEDT-TTF)$_2$Cu(SCN)$_2$ contains broad electronic features; a heavly damped Drude-like response in the far-infrared and a mid-infrared (MIR) 'hump'. Regarding the MIR 'hump' the literature only agrees to the extent that it originates from excitation across a gap in the electronic spectrum[22,34,35]. The simplest picture is to assign it to a gap in the single electron

band structure[22]. This model is improved by including electron-electron interaction effects[34]. In this case the 'hump' originates from a combination of the single electron band gap and the onsite correlation energy. Which is considered dominant, and which the perturbation, depends upon how correlated the system is believed to be. Analogously, inclusion of the electron-phonon interaction modifies the electronic spectrum. The phase-phonon model includes this explicitly as a relatively small perturbation to the band gap. In the limit of large electron-phonon coupling the strain-field is considered to localize the charge carrier[35], in which case the small polaron binding energy will be the band gap dressed by the electron-phonon interaction. All these theories share the common assumption that IR active interband electronic processes are subject to remormalization by many-body effects. In the following subsection we do not attempt to identify the origin of the renormalizations, but present evidence of their influence on the pressure dependence of the electronic contributions to the IR spectrum.

A. The pressure dependence of the carrier effective mass.

This subsection focuses on the pressure dependence of the carrier effective mass extracted from modeling with the phase-phonon theory. The plasma frequency, $\omega_{\rm p}$, parameterizes the charge carrier density, $\mathtt{N}$, and effective mass, here denoted $m^*_{\rm pp}$,

$$\omega_{\rm p}^2 = \frac{\mathtt{N}e^2}{\epsilon_0 m^*_{\rm pp}}. \qquad (25)$$

For our actual pressure range the band filling is independent of pressure and the carrier density only has a small pressure dependence arising from the reduction in unit cell parameters[2,6].

For a plasma frequency dominated by intraband processes the pressure dependence of $m^*_{\rm pp}$ arises solely from the pressure dependence of the band parameters[5,6], *i.e.* the increase in band width and curvature as the wave function overlap increases. We argue that if the plasma frequency also parameterizes the interband processes it will contain contributions from quasiparticle mass renormalization. The first point to note (see Section III C) is that the plasma frequency in the phase phonon model not only describes screening ability of the free carriers (the intraband response) but also the density of states and band curvatures associated with intraband absorption. Thus following the preceeding logic the mass $m^*_{\rm pp}$ will to some extent be renormalized by many-body effects[5].

The second point to note is that using the pressure dependence of the Raman modes to constrain the mode frequencies for the phase-phonon model significantly reduces the parameter space encountered when modeling the IR response of this system. This is not only because it eliminates the mode frequencies as free parameters, but because the softening of the modes is dependent upon the perturbation to the band gap, $\Delta - \Delta_0$. In this manner the mode frequencies provide further constraint to the parameters describing the electronic response. The parameters describing the electronic response are thus believed to have greater validity than those obtained from a simple Drude-Lorentz fit[6].

The pressure dependence of the effective masses $m^*_{\rm pp}$ obtained using the phase-phonon theory is shown in Figures 6 and 7. For both polarization directions $m^*_{\rm pp}$

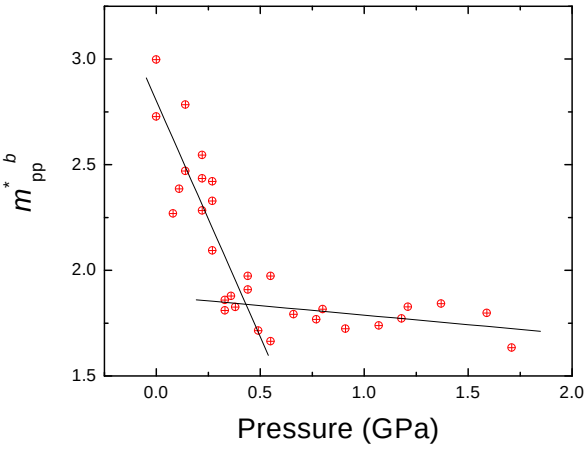


FIG. 6: The mass $m^{*\,b}_{\rm pp}$ for light polarized parallel to the b-axis, deduced from the phase-phonon fit to the optical data. For $P < 0.5$PGa, $\mathrm{d}m^{*\,b}_{\rm pp}/dP \sim -2.2\mathrm{m_e}$ and $\mathrm{dln}\, m^{*\,b}_{\rm pp}/dP \sim -80\%$/GPa. For $P > 0.5$PGa, $\mathrm{d}m^{*\,b}_{\rm pp}/dP \sim -0.9\mathrm{m_e}$ and $\mathrm{dln}\, m^{*\,b}_{\rm pp}/dP \sim -5\%$/GPa.

decreases with the application of pressure. For both polarizations this decrease is clearly nonlinear and this is highlighted by linear fits to the low (< 0.5 GPa) and high pressure regions (> 0.5 GPa)(see Fig. 6 and 7). These pressure ranges were chosen because the b-axis $m^{*\,b}_{\rm pp}$ clearly exhibits a change of slope at 0.5 GPa. The trend in $m^{*\,c}_{\rm pp}$ for polarization parallel to the c-axis is far less clear-cut. Band structure calculations giving the pressure dependence of the bare band mass[36] indicate a sublinear behaviour for its pressure dependence. However this is a much smaller correction to linear behavior than observed here and fails to reproduce the change in slope at 0.5 GPa. The coincidence of 'kinks' in the pressure dependence of $m^*_{\rm pp}$ obtained here and m^* from magnetic quantum oscillation data[2] is thus an indication that the phase-phonon fitting procedure is sensitive to many-body effects. It is these renormalizations which are known to strongly influence superconductivity in this material[2,6].

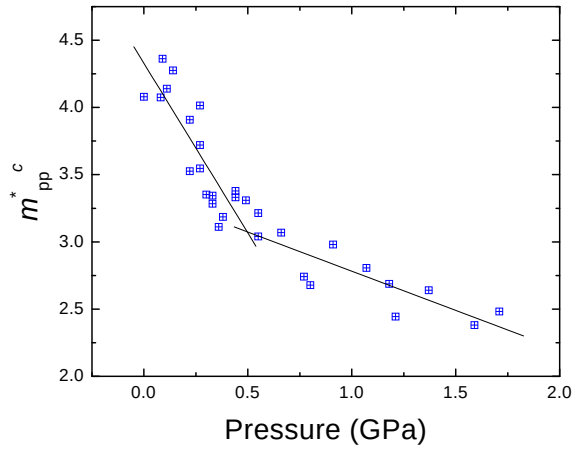


FIG. 7: The mass $m^{*\,c}_{\rm pp}$ for light polarized parallel to the c-axis, deduced from the phase-phonon fit to the optical data. For $P < 0.5$PGa, $\mathrm{d}m^{*\,c}_{\rm pp}/dP \sim -2.5\mathrm{m_e}$ and $\mathrm{dln}\, m^{*\,c}_{\rm pp}/dP \sim -58\%$/GPa. For $P > 0.5$PGa, $\mathrm{d}m^{*\,c}_{\rm pp}/dP \sim -0.6\mathrm{m_e}$ and $\mathrm{dln}\, m^{*\,c}_{\rm pp}/dP \sim -17\%$/GPa.

B. Implications for the superconducting pairing mechanism.

It has been shown previously[37] that the usual electron-acoustic phonon interaction mechanism is unable to account for the magnitude of the electron-phonon coupling constant or the large pressure dependence of $T_{\rm c}$ in the BEDT-TTF superconductors. A further refinement[37] includes the attractive interaction mediated by the A_g molecular modes, with the total electron-phonon coupling constant, $\lambda_{\rm TOT}$, given by a Yamaji sum over the individual A_g molecular modes. The energy scale for the interaction is set by the Debye frequency, Θ[37,38]. Caulfield *et al.*[2] have previously inferred $\Theta \approx 40\mathrm{cm}^{-1}$ by fitting the effective mass dependence of $T_{\rm c}$ with a linearised Eliashberg equation using an Einstein density of phonon states, $\delta(\Theta)$. High and low temperature specific heat measurements[39,40] yield values of Θ ranging from $38\mathrm{cm}^{-1}$ to $140\mathrm{cm}^{-1}$. Calculations of $\lambda_{\rm TOT}$[37] give values ranging from 0.25-0.45[41,42,43].

The weak-coupling BCS formula[44] gives a satisfactory functional description of the ambient pressure $T_{\rm c}$[10] and describes the effective mass dependence of the superconducting transition temperature[2].However, the fact that the weak-coupling BCS expression describes $T_{\rm c}$ versus m^* well[2] should NOT be taken to imply that κ-(BEDT-TTF)$_2$Cu(SCN)$_2$ is a weak-coupling BCS superconductor. The formula is used here as a convenient parameterization which is known to describe earlier data well[2,45].

The pressure derivative of the weak-coupling BCS formula provides a convenient parametrization of $\frac{\mathrm{d}\ln\, T_{\rm c}}{\mathrm{d}P}$ in terms of $\frac{\mathrm{d}\lambda}{\mathrm{d}P}$,

$$\frac{\mathrm{d}\ln\, T_{\rm c}}{\mathrm{d}P} = \frac{\mathrm{d}\ln\Theta}{\mathrm{d}P} + \frac{1}{(\lambda-\mu^*)^2}\left[\frac{\mathrm{d}\lambda}{\mathrm{d}P} - \frac{\mathrm{d}\mu^*}{\mathrm{d}P}\right]. \qquad (26)$$

With

$$\frac{1}{(\lambda-\mu^*)^2} = \left[\ln\left(\frac{T_{\rm c}}{1.13\Theta}\right)\right]^2, \qquad (27)$$

$\Theta \approx 90\pm50$ cm^{-1} [2,39,40] and using the average pressure-induced stiffening of the Raman active lattice modes of $\approx +13$ %GPa^{-1} [9] for $\frac{\mathrm{d}\ln\Theta}{\mathrm{d}P}$, the only unknown is the pressure dependence of the Coulomb pseudopotential, $\frac{\mathrm{d}\mu^*}{\mathrm{d}P}$. There is sufficient uncertainty in the calculations of μ^* that an accurate estimate for its pressure dependence cannot be made[46]. However, μ^* is known to scale with the density of states at the Fermi energy[46], which will decrease with the application of pressure[2]. Thus if μ^* is positive[42] it will decrease with pressure and omitting $\frac{\mathrm{d}\mu^*}{\mathrm{d}P}$ from Equation 26 will result in an overestimate for the rate of suppression of $T_{\rm c}$ with pressure. A negative value of μ^* indicates that direct (non phonon-mediated) electron-electron interactions are involved in the pairing[2,46] which are not measured by these experiments. Consequently $\frac{\mathrm{d}\mu^*}{\mathrm{d}P}$ is ignored in Equation 26.

Estimates for the pressure dependence of the electron-phonon coupling constant, based on the vibrations sampled and the two methods of calculation are used to calculate the right-hand side of Equation 26. It should be emphasized that the two models we are employing to estimate the pressure dependence of the electron-phonon coupling constant lie at opposite limits of our sample's behaviour, the dimer charge-oscillation model being the limit of a localized electronic system and the phase-phonon model the limit of an itinerant system. A conclusion common to both methods of analysis should thus be a robust one.

1. $T_{\rm c}(P)$ *from the dimer charge-oscillation model.*

Employing the dimer charge model, $\lambda_{\rm TOT}$ is assumed to have a pressure dependence similar to that of the strongly coupled C=C mode, *i.e.* of the order of -17 %GPa^{-1}, with an upper limit of -20%GPa^{-1} used in this calculation. This gives $\frac{\mathrm{d}\ln\, T_{\rm c}}{\mathrm{d}P} \approx$ -40$\pm$32 %GPa^{-1}, which is far from the experimentally observed value of $\frac{\mathrm{d}\ln\, T_{\rm c}}{\mathrm{d}P} \approx$ -200 %GPa^{-1} [2,3].

As can be seen from (27), Θ logarithmically scales with the dependence of the pressure derivative of $T_{\rm c}$ on the pressure derivative of the coupling constant. Thus to obtain the observed rapid fall of $T_{\rm c}$ with pressure from only the decrease in the electron-phonon coupling constant requires Θ to be of the order of the C=C mode frequency, $\approx$ 1500 cm^{-1}. Such a value is inconsistent with the 10 K superconducting temperature and the unconventional isotope shift observed upon carbon substitution[47].

Thus, the electron-phonon coupling as extracted from the dimer-charge-oscillation model cannot be the relevant parameter for superconductivity in our organic superconductor.

2. $T_c(P)$ from the phase-phonon model.

The pressure dependence of the electron-phonon coupling constant derived from the phase-phonon model provides far less clear-cut results. In this case λ_{TOT} is assumed to have a pressure dependence of -40±20 %GPa^{-1}, a value consistent with the phase-phonon calculation of λ for all observed modes. This gives $\frac{\mathrm{d}\ln\ T_c}{\mathrm{d}P} \approx$ -90 %GPa^{-1} with the asymmetric error of +150 and -77 %GPa^{-1}. The upper bound of this estimate is close to the experimentally observed value of $\frac{\mathrm{d}\ln\ T_c}{\mathrm{d}P} \approx$ -200 %GPa^{-1} [2,3]. Thus, the upper estimate of all parameters would be required to explain the pressure dependence of $T_c(P)$ as arising solely due to a reduction in the electron-phonon coupling constant.

3. Comparison.

Again, it should be stressed that the dimer charge-oscillation model represents the limit of localized electronic behaviour and the phase-phonon model represents the limit of itinerant electronic behaviour. The true properties of κ-(BEDT-TTF)$_2$Cu(SCN)$_2$ under these experimental conditions are believed to lie somewhere between these extremes. Both models have similar conclusions , *i.e.* $\frac{\mathrm{d}\ln\ T_c}{\mathrm{d}P}$ cannot be reproduced within weak coupling BCS theory. The fact that the similar conclusions are drawn when employing either model suggests that they are robust.

Use of the dimer charge-oscillation model casts considerable doubt on whether this material is a simple BCS superconductor because the characteristic energy of the pairing interaction would have to be of the order of the highest frequency molecular modes, a value inconsistent with the 10 K superconducting transition temperature. However this conclusion must be treated with caution due to the numerous assumptions involved in applying this model of a localized system to the coupling between the molecular vibrations and delocalized conduction electrons. Doubt on whether this material is a simple BCS superconductor is also cast by the application of the phase-phonon model, because the upper estimate of all parameters is required to explain the experimentally observed suppression of T_c with pressure.

This indicates that electron-electron interaction may be playing a significant role in this material's superconducting mechanism. It is worth noting that there is mounting evidence in support of this conclusion. Both experimental[48,49] and theoretical[50], studies predict that the superconducting order parameter in this material has an 'exotic' d-wave symmetry, a property predicted for a superconducting state whose pairing is mediated by spin fluctuations[50,51], *i.e.* direct electron-electron interaction[1].

V. CONCLUSIONS.

Comparison of high-pressure Raman scattering and infrared reflectivity data provides an alternative method for probing the quasiparticle contributions to effective mass enhancement known to be intimately connected to superconductivity in this material[2]. It also enables the pressure dependence of the electron-phonon coupling strength to be evaluated for modes observed in both spectra. Using the weak coupling limit of BCS theory the pressure dependence of the electron-phonon coupling constant is compared to the pressure dependence of the superconducting transition temperature. This casts doubt on whether this material is a simple BCS superconductor, an indication that electron-electron interaction may be playing a significant role in this material's superconducting mechanism.

VI. ACKNOWLEDGEMENTS

The authors would like to thank A. P. Jephcoat and H. Olijnyk from the Earth Science Department, Oxford University, UK and A. F. Goncharov, V. V. Struzhkin, Hokwang Mao and R. J. Hemley from the Geophysical Laboratory, Carnegie Institute, Washington, USA for their stimulating collaboration that resulted in the measurements[6,9] that the analysis in this paper is based upon. This work is supported by the EPSRC (UK).

* rmcd@lanl.gov; Ross McDonald would like to thank Drs. Neil Harrison, Charles Mielke and Albert Miglori for stimulating and fruitful discussions.

[1] J. Singleton, Rep. Prog.Phys. **63**, 1111 (2000). J. Singelton and C. H. Mielke, Contemp. Phys. **43**, 63 (2002).
[2] J. Caulfield, W. Lubczynski, F. Pratt, J. Singelton, D. Ko, W. Hayes, M. Kurmoo, and P. Day, J. Phys.:Condens. Matter **6**, 2911 (1994).
[3] K. Murata, Y. Honda, H. Anxai, M. Tokumoto, K. Takahashi, N. Kinshita, and T. Ishiguro, Synth. Metals **27**, A263 (1989).
[4] N. Harrison, J. Caulfield, J. Singleton, P. H. P. Reinders, F. Herlach, W. Hayes, M. Kurmoo, P. Day, J. Phys.: Condens. Matter **8**, 5415 (1996).
[5] A. Legget, Annals of physics **46**, 76 (1968).
[6] A.-K. Klehe, R. McDonald, A. Goncharov, V. Struzhkin, H. Mao, R. Hemley, T. Sasaki, W. Hayes, and J. Singleton, J. Phys.: Condens. Matter **12**, L247 (2000).

[7] In this paper we extract an effective mass from the optical data that is strongly influenced by interband electronic processes. We argue that in contrast to the intraband processes the interband ones are renormalized by quasi-particle interactions, see Subsection IV A.

[8] Polarized IR refectance measurement were performed in the highly conductive, crystallographic *bc*-plane of the crystal with the electric field polarized parallel to the crystallographic *b*- or crystallographic *c*-axis, respectively.

[9] R. McDonald, A.-K. Klehe, A. Jephcoat, H. Olijnyk, T. Sasaki, W. Hayes, and J. Singleton, J. Phys.: Condens. Matter. **13**, L291 (2001).

[10] T. Sugano, H. Hayashi, M. Kinoshita, and K. Nishikida, Phys. Rev. B **39**, 11387 (1989).

[11] K. Kornelsen, J. Eldridge, H. Wang, and J. Williams, Solid state commun. **72**, 475 (1989).

[12] M. Rice, Solid state commun. **31**, 93 (1979).

[13] J. Eldridge, C. Homes, J. Williams, A. Kini, and H. Wang, Spectrochim. Acta A **51A**, 947 (1995).

[14] R. McDonald, A.-K. Klehe, J. Singleton, and W. Hayes, Synth. Metals **in press**, (2001).

[15] R. Zallen, Phys. Rev. B **9**, 4485 (1974).

[16] V. Yartsev and A. Graja, Int. J. Mod. Phys. B **12**, 1643 (1998).

[17] M. Rice, Phys. Rev. Lett. **37**, 36 (1976).

[18] V. Yartsev and A. Graja, J. Phys.: Condens. Matter **2**, 9631 (1990).

[19] M. Rice and V. Y. anfd C.S. Jacobsen, Phys. Rev. B **21**, 3437 (1979).

[20] Bozio, Meneghetti, and Pecile, J. Chem. Phys. **79**, 5793 (1982).

[21] M. Rice, L. Pietronero, and P. Brüesch, Solid state commun. **21**, 757 (1977).

[22] K. Kornelsen, J. Eldridge, H. Wang, and J. Williams, Phys. Rev. B **44**, 5235 (1991).

[23] M. Kozlov and M. Tokumoto, Synth. Metals **70**, 1023 (1995).

[24] J. Inkson, *Many-body theory of solids* (Penum, 1984).

[25] H. Haken, *Quantum field theory of solids* (North-Holland, 1976).

[26] D. Pines and P. Nozieres, *The theory of quantum liquids* (Benjamin, 1966), Vol. 1.

[27] R. Kubo, Can. J. Phys **34**, 1274 (1956).

[28] D. Pines, *The many-body problem* (Benjamin, 1962).

[29] A. Panelli, A. Girlando, and C. Pecile, Solid state commun. **52**, 801 (1984).

[30] M. Dove, *Introduction to lattice dynamics* (Cambridge university press, 1993).

[31] P. Lee, M. Rice, and P. Anderson, Solid state commun. **14**, 703 (1974).

[32] E. Fenton and G.C.Psaltakis, Solid state commun. **47**, 767 (1983).

[33] The electronic contributions to the spectra are not accurately reproduced using a single frequency independent value for the electronic damping.

[34] J. Merino and R. McKenzie, Comments Cond. Matt. Phys. **18**, 309 (1998).

[35] N. Wang, B. Clayman, H. Mori, and S. Tanaka, Physica C **341**, 2225 (2000).

[36] R. McDonald, to be published (2002).

[37] K. Yamaji, Solid state commun. **61**, 413 (1986).

[38] J. Faulhaber, D. Ko, and P. Briddon, Synth. Metals **60**, 227 (1993).

[39] N. Fortune, G. Rajaram, and K. Murata, Synth. Metals **103**, 2080 (1999).

[40] B. Andraka, J. Kim, G. Stewart, K. Carlson, H. Wang, and J.M.Williams, Phys. Rev. B **40**, R11345 (1998).

[41] S. Hill, Synth. Metals **55-57**, 2566 (1993).

[42] J. Shumway, S. Chattopadhyay, and S. Satpathy, Phys. Rev. B **53**, 6677 (1996).

[43] O. Drozdova, V. Semkin, R. Vlasova, N. Kushch, and E. Yagubskii, Synth. Metals **64**, 17 (1994).

[44] J. Bardeen, L. Cooper, and J. Schrieffer, Phys. Rev. **108**, 1175 (1957).

[45] J. Caulfield, W. Lubczynski, W. Lee, J. Singelton, F. Pratt, W. Hayes, M. Kurmoo, and P. Day, Synth. Metals **70**, 185 (1995).

[46] W. Lee, Solid state commun. **106**, 601 (1998).

[47] J. Schlueter, A. Kini, B. Ward, U. Geiser, H. Wang, J. Mohtasham, R. Winter, and G. Gard, Physica C **351**, 261 (2001).

[48] K. Izawa, H. Yamaguchi, T. Sasaki, and Y. Matsuda, Phys. Rev. Lett **88**, 027002 (2002).

[49] T. Arai, K. Ichimura, S. Takasaki, J. Y. S. Nakatsuji, and H. Anzai, Phys. Rev. B **63**, 104518 (2001).

[50] K. Kuroki, T. Kimura, R. Arita, Y. Tanaka, and Y. Matsuda, Xarcive (2001).

[51] J. Annett, Contemporary Physics **36**, 423 (1995).